Article

Cell
PRESS

RGS4 Is Required for Dopaminergic Control of Striatal LTD and Susceptibility to Parkinsonian Motor Deficits

Talia N. Lerner[1,3] and Anatol C. Kreitzer[1,2,3,*]

[1]Gladstone Institute of Neurological Disease
[2]Departments of Physiology and Neurology
[3]Neuroscience Graduate Program
University of California, San Francisco, San Francisco, CA 94158, USA
*Correspondence: akreitzer@gladstone.ucsf.edu

SUMMARY

Plasticity of excitatory synapses onto striatal projection neurons (MSNs) has the potential to regulate motor function by setting the gain on signals driving both direct- and indirect-pathway basal ganglia circuits. Endocannabinoid-dependent long-term depression (eCB-LTD) is the best characterized form of striatal plasticity, but the mechanisms governing its normal regulation and pathological dysregulation are not well understood. We characterized two distinct signaling pathways mediating eCB production in striatal indirect-pathway MSNs and found that both pathways were modulated by dopamine D2 and adenosine A2A receptors, acting through cAMP/PKA. We identified regulator of G protein signaling 4 (RGS4) as a key link between D2/A2A signaling and eCB mobilization pathways. In contrast to wild-type mice, RGS4$^{-/-}$ mice exhibited normal eCB-LTD after dopamine depletion and were significantly less impaired in the 6-OHDA model of Parkinson's disease. Taken together, these results suggest that inhibition of RGS4 may be an effective nondopaminergic strategy for treating Parkinson's disease.

INTRODUCTION

The basal ganglia are a network of subcortical brain nuclei engaged in many aspects of motor function, including action selection and adaptive motor learning (Graybiel et al., 1994; Hikosaka et al., 2000; Packard and Knowlton, 2002; Yin and Knowlton, 2006). Information enters the basal ganglia through the striatum, whose principal neurons (medium spiny neurons [MSNs]) receive highly convergent excitatory input from the cortex and thalamus (Bolam et al., 2000). The excitatory synapses formed onto MSNs are an important site of long-term plasticity in the basal ganglia network (Kreitzer and Malenka, 2008; Lerner and Kreitzer, 2011; Surmeier et al.,

2009). This plasticity has the potential to powerfully regulate basal ganglia circuit function, and therefore motor function, by setting the gain on incoming cortical and thalamic signals. Defects in striatal plasticity are thought to play a role in many movement disorders, including Parkinson's disease, Huntington's disease, and dystonia (Kitada et al., 2007, 2009; Kreitzer and Malenka, 2007; Kurz et al., 2010; Peterson et al., 2010; Shen et al., 2008).

Despite its functional importance, the molecular mechanisms underlying striatal plasticity remain elusive. The best-studied form of striatal plasticity is endocannabinoid-dependent LTD (eCB-LTD). This form of LTD is induced following the production and release of endocannabinoids (eCBs) from the postsynaptic neuron, which then act on presynaptic CB1 receptors to lower neurotransmitter release probability. Although eCB-LTD is observed in both subtypes of MSNs (Shen et al., 2008), it can be most reliably induced in vitro at excitatory synapses onto indirect-pathway MSNs (Kreitzer and Malenka, 2007), which express dopamine D2 and adenosine A2A receptors. There are several postsynaptic membrane proteins that are required to elicit eCB release sufficient to induce indirect-pathway eCB-LTD: group I (G$_q$-coupled) metabotropic glutamate receptors (mGluRs), L-type voltage-gated calcium channels (L-VGCCs), and dopamine D2 receptors (Calabresi et al., 1994, 1997; Choi and Lovinger, 1997; Kreitzer and Malenka, 2005; Sung et al., 2001). Adenosine A2A receptors are also able to modulate indirect-pathway LTD (Lerner et al., 2010; Shen et al., 2008). Previous work has established the importance of postsynaptic activation of group I mGluRs and L-VGCCs (Calabresi et al., 1994; Choi and Lovinger, 1997; Sung et al., 2001), yet it is not known how the signaling pathways of these two membrane proteins interact. It has also been proposed that phospholipase Cβ (PLCβ) is a coincidence detector for group I mGluR activation of G$_q$ signaling and calcium influx through L-VGCCs (Fino et al., 2010; Hashimotodani et al., 2005). However, the precise role of PLCβ in striatal eCB-LTD is not clear (Adermark and Lovinger, 2007).

Similarly, it remains unclear why activation of D2 receptors is required for eCB-LTD and blockade of A2A receptors enhances it. One study indicated that D2 receptors act via adenylyl cyclase 5 (Kheirbek et al., 2009), but what occurs downstream of cAMP production is not known. Other studies have

questioned whether the D2 receptors that modulate LTD are located on MSNs or on cholinergic interneurons (Tozzi et al., 2011; Wang et al., 2006).

Understanding how dopamine receptors control striatal function is especially important in the context of Parkinson's disease, where dopaminergic input to the striatum is lost. For many decades, Parkinson's patients have been treated with the dopamine precursor levodopa and more recently with dopamine receptor agonists (typically D2-receptor-specific agonists). While this direct approach of dopamine replacement is extremely helpful in relieving symptoms early in the disease process, as the disease progresses its efficacy wanes and side effects often develop. A better understanding of how dopamine acts in the striatum could lead to new strategies for treating Parkinson's disease symptoms downstream of dopamine receptors.

Ultimately, the signaling pathways of group I mGluRs, L-VGCCs, D2 receptors and A2A receptors must converge to control the postsynaptic mobilization of eCBs. However, the specific pathways underlying eCB mobilization for striatal LTD—and the putative eCB produced—are not clear. There are two major candidates for the eCB produced: (1) anandamide (AEA), thought to be produced by phospholipase D (PLD) activity, and (2) 2-arachidonoylglycerol (2-AG), thought to be produced by PLCβ and DAG lipase (Ahn et al., 2008; Piomelli, 2003). Much of the available evidence has supported the role of AEA in indirect-pathway LTD (Ade and Lovinger, 2007; Giuffrida et al., 1999; Kreitzer and Malenka, 2007). However, 2-AG can also mediate LTD (Fino et al., 2010; Lerner et al., 2010). Additionally, 2-AG appears to be the major signaling eCB for plasticity in other brain areas, as well as for short-term eCB-dependent plasticity in the striatum (Gao et al., 2010; Tanimura et al., 2010; Uchigashima et al., 2007).

In this study, we outline a model of striatal eCB production that clarifies the role of group I mGluRs, internal calcium stores, and L-VGCCs during LTD induction by both low- and high-frequency stimulation protocols. We also provide a mechanism for the control of eCB production by D2 and A2A receptors in striatal MSNs. Specifically, we find that a GTPase-activating protein called regulator of G protein signaling 4 (RGS4) links D2 and A2A signaling to group I mGluR signaling. These findings unify a number of previously disparate findings related to striatal eCB-LTD, and raise the possibility of new nondopaminergic drugs to treat Parkinson's disease.

RESULTS

PLCβ-Dependent and -Independent Forms of eCB-LTD Can Be Elicited at Excitatory Synapses onto Striatal Indirect-Pathway MSNs

To study the mechanisms of eCB-LTD in indirect-pathway MSNs, we began by confirming that high-frequency stimulation (HFS; 100 Hz) of excitatory afferents to indirect-pathway MSNs in the dorsolateral striatum causes eCB-LTD when paired with postsynaptic depolarization (48% ± 2% of baseline at 30–40 min in control conditions; 97% ± 6% in the cannabinoid CB1 receptor antagonist AM251; p < 0.05; Figures 1A and 1B). We also confirmed that HFS-LTD is dependent on group I

(G_q-coupled) mGluRs by bath application of the group I mGluR antagonist AIDA (96% ± 12%, p < 0.05 compared to control; Figure 1C). Next, we tested potential signaling pathways downstream of G_q. The canonical target of G_q is PLCβ (Hubbard and Hepler, 2006; Taylor et al., 1991). Surprisingly, we were unable to block HFS-LTD by including the PLC inhibitor U73122 in the intracellular recording solution (54% ± 5%; Figure 1C). This finding was unexpected because other groups have demonstrated that eCB-mediated depression in MSNs is PLCβ-dependent (Fino et al., 2010; Hashimotodani et al., 2005; Jung et al., 2005; Yin and Lovinger, 2006) although not in all cases (Adermark and Lovinger, 2007). Therefore, we decided to examine whether the PLCβ-independence of HFS-LTD was unique to that stimulation protocol.

As an alternative to HFS-LTD, we applied a low-frequency stimulation (LFS) induction protocol that is qualitatively similar to that used in previous studies of striatal LFS-LTD (Lerner et al., 2010; Ronesi and Lovinger, 2005). In brief, we repeatedly paired epochs of 20 Hz stimulation with postsynaptic depolarization over several minutes (see Experimental Procedures for details) to induce LTD (56% ± 10%; Figures 1D and 1E). Similar to HFS-LTD, LFS-LTD was blocked by AM251 and AIDA (95% ± 6% in AM251; 100% ± 8% in AIDA; both p < 0.05 compared to control; Figures 1E and 1F), indicating a dependence on CB1 receptors and group I mGluRs, respectively. However, LFS-LTD was also blocked by intracellular U73122 (102% ± 15%; p < 0.05 compared to control; Figure 1F), indicating a role for PLCβ. Thus, both PLCβ-dependent and -independent forms of eCB-LTD can be elicited at excitatory synapses onto striatal indirect-pathway MSNs simply by using different stimulation frequencies and repetitions.

LFS-LTD Requires DAG Lipase But Not Elevations in Intracellular Calcium

PLCβ is an enzyme that produces the intracellular secondary messenger diacylglycerol (DAG), which can be converted to the eCB 2-arachidonylglycerol (2-AG) by the enzyme DAG lipase (DAGL). The sequential activities of PLCβ and DAGL represent a well-defined pathway for 2-AG production that could mediate LFS-LTD. To test whether DAGL is also required for LFS-LTD, we applied the LFS-LTD induction protocol in the presence of the DAGL inhibitor THL and observed that THL blocked LFS-LTD (92% ± 13%; p < 0.05 compared to control; Figure 2A).

In addition to DAG, PLCβ produces another important secondary messenger, IP_3, which can activate IP_3 receptors located on the endoplasmic reticulum and cause release of calcium from internal stores. To test whether internal calcium stores are involved in LFS-LTD, we added thapsigargin, which depletes these stores, to our intracellular recording solution, but this manipulation did not block LFS-LTD (47% ± 7%; Figure 2B).

Although internal calcium stores were not required for LFS-LTD, other sources of calcium might be important. L-type voltage-gated calcium channels (L-VGCCs) have previously been implicated in eCB release (Adermark and Lovinger, 2007; Calabresi et al., 1994; Choi and Lovinger, 1997; Kreitzer and Malenka, 2005), yet we found that the L-VGCC blocker nitrendipine did not block LFS-LTD (64% ± 6%; Figure 2C). Another
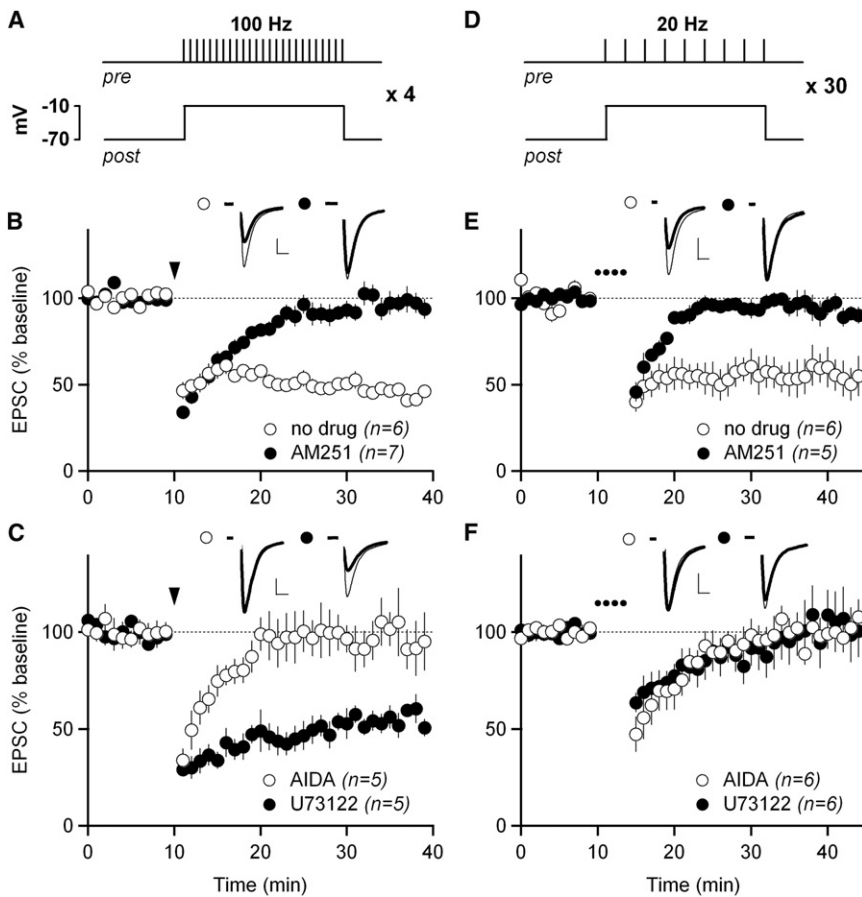
Figure 1. PLCβ-Dependent and -Independent Forms of eCB-LTD Can Be Elicited at Excitatory Synapses onto Striatal Indirect-Pathway MSNs

(A) Schematic of the high-frequency stimulation (HFS)-LTD induction protocol. One hundred hertz stimulation for one second was paired with postsynaptic depolarization to −10mV. This stimulation was repeated four times at ten second intervals.

(B) HFS-LTD in control conditions (white circles) and in 1 μM of the CB1R antagonist AM251 (black circles). In this, and all subsequent panels showing LTD, normalized EPSC amplitudes are plotted over time. Traces from representative experiments are shown above the graph. The thin traces show the average EPSC from 0–10 min, and the thick traces show the average EPSC from 30–40 min. For HFS-LTD, the arrowhead indicates the time of induction. In all panels, scale bars are 100 pA × 5 ms and error bars are SEM.

(C) HFS-LTD in 100 μM of the mGluR1/5 antagonist AIDA (white circles) and with 10 μM of the PLCβ inhibitor U73122 included in the intracellular pipette solution (black circles).

(D) Schematic of the low-frequency stimulation (LFS)-LTD induction protocol. Twenty hertz stimulation for one second was paired with postsynaptic depolarization to −10mV. This stimulation was repeated 30 times at ten second intervals to induce LFS-LTD.

(E) LFS-LTD in control solution (white circles) and in 5 μM AM251 (black circles). In all panels showing LFS-LTD, the dotted line indicates the time of LFS-LTD induction.

(F) LFS-LTD in 100 μM AIDA (white circles) and with 10 μM U73122 included in the intracellular solution (black circles).

L-VGCC blocker, nifedipine, also did not block LFS-LTD (64% ± 10%, n = 6, data not shown). In fact, elevations in intracellular calcium do not appear to be strictly required for LFS-LTD, since loading MSNs with the calcium-chelator BAPTA did not block LFS-LTD (75% ± 10%; Figure 2C). From these experiments, we conclude that the most likely scenario for LFS-LTD induction is that activation of G_q-coupled mGluRs leads to activation of PLCβ, stimulating the production of DAG, which is then converted to 2-AG by DAGL (Figure 2D).

HFS-LTD Requires Elevations in Intracellular Calcium-Mediated by L-type Calcium Channels and Calcium-Induced Calcium Release

Our initial experiments (Figure 1) showed that the pathways underlying HFS-LTD and LFS-LTD diverge after just one step in their induction pathways (activation of G_q by group I mGluRs). Because HFS-LTD is PLCβ-independent (Figure 1C), we predicted it would be DAGL-independent as well. Indeed, as observed previously (Ade and Lovinger, 2007; Lerner et al., 2010), the DAGL inhibitor THL did not block HFS-LTD (61% ± 10%; Figure 3A). We also tested whether HFS-LTD differed from LFS-LTD in its requirements for calcium. By adding thapsigargin to our intracellular solution to deplete internal calcium stores, we found that, unlike LFS-LTD, HFS-LTD requires these stores (117% ± 17%; p < 0.05 compared to control; Figure 3B). Calcium from internal stores can be released into the cytoplasm via either IP_3 receptors or ryanodine receptors (RyRs). Since HFS-LTD does not require PLCβ, which produces IP_3, we reasoned that the requirement for internal calcium stores in HFS-LTD was more likely to be dependent on RyRs than on IP_3 receptors. Indeed, when RyRs were inhibited by including ryanodine in the intracellular solution, HFS-LTD was blocked (108% ± 8%; p < 0.05 compared to control; Figure 3B). An IP_3 receptor blocker, 2-APB, did not block HFS-LTD when included in the intracellular solution (63% ± 10%; Figure S2A available online).

RyRs are activated by calcium and, once activated, cause the release of more calcium into the cytoplasm. This process of calcium-induced calcium release (CICR) serves to amplify calcium signals initiated by other sources of calcium influx. What is the CICR-initiating source of calcium in HFS-LTD? We consider L-VGCCs to be a likely source, because they are functionally coupled to RyRs (Chavis et al., 1996) and because L-VGCCs have previously been shown to be involved in striatal LTD (Calabresi et al., 1994; Choi and Lovinger, 1997). In agreement with this hypothesis, the L-VGCC antagonist nitrendipine blocked HFS-LTD (92% ± 4%; p < 0.05 compared to control; Figure 3C).
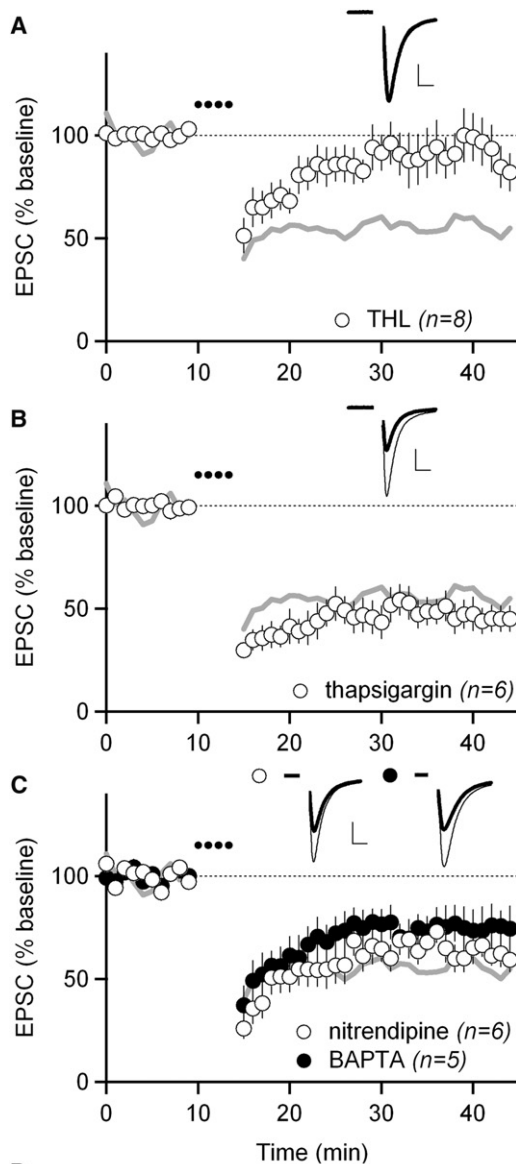
Figure 2. LFS-LTD Requires Diacylglycerol Lipase But Not Elevations In Intracellular Calcium

(A) LFS-LTD in 10 μM of the diacylglycerol lipase inhibitor THL. Gray traces in (A), (B), and (C) show control LFS-LTD from Figure 1E for reference. In all panels, scale bars are 100 pA × 5 ms and error bars are SEM.

(B) LFS-LTD with 10 μM of the intracellular calcium store depleter thapsigargin included in the intracellular solution.

(C) LFS-LTD with 10 μM of the L-type calcium channel blocker nitrendipine (white circles) and with 10 μM of the calcium chelator BAPTA (black circles) included in the intracellular solution.

(D) Schematic showing the proposed signaling pathway underlying LFS-LTD. Activation of G_q-coupled mGluRs activates PLCβ, stimulating the production of diacylglycerol (DAG), which is then converted to the endocannabinoid 2-arachidonoylglycerol (2-AG) by diacylglycerol lipase (DAGL).

HFS-LTD Requires Src Kinase and Phospholipase D

Why does HFS-LTD require group I mGluRs if it is PLCβ-independent? We reasoned that G_q must activate another enzyme in addition to PLCβ. Other direct targets of G_q include nonreceptor tyrosine kinases (Bence et al., 1997). Src-family kinases are nonreceptor tyrosine kinases that phosphorylate a number of targets linked to eCB mobilization, including L-type calcium channels and phospholipase D (PLD; Bence-Hanulec et al., 2000; Henkels et al., 2010). Therefore, to test whether Src-family kinases are required for HFS-LTD, we attempted to induce HFS-LTD in the presence of the Src-family kinase inhibitor PP2. PP2 completely blocked HFS-LTD (105% ± 16%; p < 0.05 compared to control; Figure 3D). To further test the hypothesis that postsynaptic Src, specifically, is required for HFS-LTD, we next included a membrane impermeable c-Src inhibitor peptide in our intracellular recording solution. This inhibitor peptide was also able to block HFS-LTD (88% ± 5%; p < 0.05 compared to control; Figure 3D). Notably, the Src inhibitor PP2 did not block LFS-LTD (62% ± 3%; Figure S1A), indicating that Src acts specifically in HFS-LTD induction.

We next explored whether Src activation and the rise in intracellular calcium due to L-VGCCs and CICR could be connected to any of the known or posited PLCβ-independent eCB production pathways. Since we had already observed that inhibiting the major 2-AG production enzyme DAGL did not block HFS-LTD (Figure 3A), we explored a possible role for enzymes proposed to mediate anandamide (AEA) biosynthesis. AEA can be produced by a number of different synthesis pathways. Key enzymes in these various pathways include PLC, PLA_2, and PLD (PLD1, PLD2, or NAPE-specific PLD; Ahn et al., 2008). A role for any PLC isoforms had already been ruled out by our experiments with the general PLC inhibitor U73122 (Figure 1C). A PLA_2 inhibitor, OBAA, also did not prevent HFS-LTD (57% ± 1%; Figure S2B). Finally, mice lacking NAPE-specific PLD have intact AEA levels (Leung et al., 2006), arguing against an essential role of that PLD isoform. However, an inhibitor of PLD (with some specificity for PLD2 over PLD1), CAY10594, significantly blocked HFS-LTD (82% ± 5%; p < 0.05 compared to control; Figure 3E). Another PLD inhibitor, CAY10593, also blocked HFS-LTD to a similar degree (85% ± 10%, n = 3, data not shown). We conclude that PLD is a key enzyme for eCB mobilization in response to HFS. These data lead us to propose a model for HFS-LTD in which activation of G_q-coupled mGluRs leads to activation of Src, stimulating the production
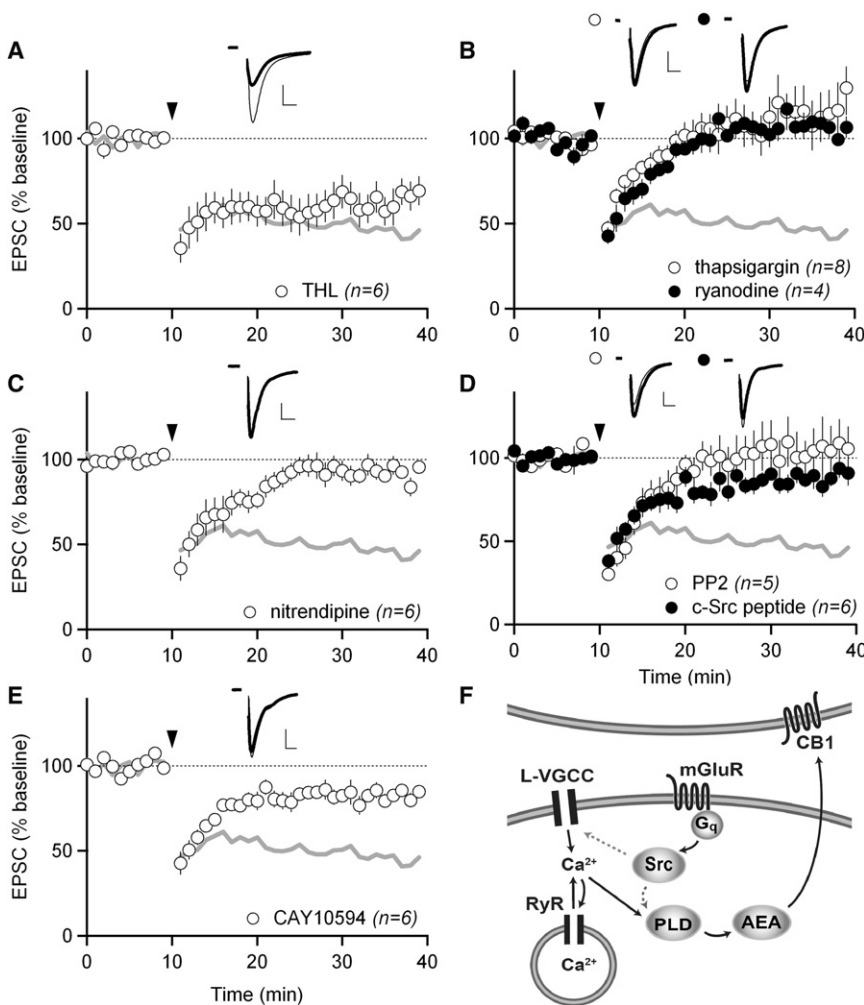
Figure 3. HFS-LTD Depends on a Distinct Signaling Pathway, Involving Src Kinase, Internal Calcium Stores, L-type Calcium Channels, and Phospholipase D

(A) HFS-LTD in 10 μM of the diacylglycerol lipase inhibitor THL. Gray traces in (A)–(E) show control HFS-LTD from Figure 1B for reference. In all panels, scale bars are 100 pA × 5 ms and error bars are SEM.

(B) HFS-LTD with 10 μM of the intracellular calcium store depleter thapsigargin included in the intracellular solution (white circles) and with 10 μM ryanodine included in the intracellular solution to specifically block ryanodine receptors (black circles).

(C) HFS-LTD in 10 μM of the L-type calcium channel blocker nitrendipine.

(D) HFS-LTD in 10 μM of the Src-family kinase inhibitor PP2 (white circles) and with 100 μM c-Src inhibitory peptide included in the intracellular solution (black circles).

(E) HFS-LTD with 100 μM of the phospholipase D (PLD) inhibitor CAY10594 (white circles).

(F) Schematic showing the proposed signaling pathway underlying HFS-LTD. Activation of G_q-coupled mGluRs activates Src, which phosphorylates and activates L-type calcium channels and/or PLD. Calcium influx through L-type calcium channels (amplified by RyR-mediated calcium-induced calcium release from internal stores) also activates PLD. PLD activity leads to the production and release of the endocannabinoid anandamide (AEA).

of AEA by PLD, either by modulating PLD function directly (Henkels et al., 2010) or by modulating L-VGCCs (Bence-Hanulec et al., 2000; Figure 3F).

Dopamine D2 and Adenosine A2A Receptors Modulate Both LFS- and HFS-LTD

Because HFS-LTD and LFS-LTD are mediated by distinct signaling pathways downstream of G_q, we wondered whether they are both modulated by dopamine D2 or adenosine A2A receptors. It is established that HFS-LTD in indirect-pathway MSNs requires dopamine D2 receptors (Kreitzer and Malenka, 2007; Shen et al., 2008). However, D2 receptor activation alone is not sufficient to induce eCB signaling; coincident group I mGluR activation is required (Figure S3). We confirmed that the D2 receptor antagonist sulpiride blocked HFS-LTD (103% ± 8%; p < 0.05 compared to control; Figure 4A). Interestingly, sulpiride was also able to inhibit LFS-LTD (88% ± 4%; p < 0.05 compared to control; Figure 4B), indicating that D2 receptors act on eCB-LTD at or upstream of G_q.

Adenosine A2A receptors are also highly expressed in indirect-pathway MSNs, where they influence eCB signaling and act in opposition to D2 receptors (Shen et al., 2008; Tozzi et al., 2007). Therefore, we tested whether activation of A2A receptors could block HFS- or LFS-LTD. The A2A receptor agonist CGS21680 blocked both HFS- and LFS-LTD (102% ± 7%; p < 0.05 compared to control for HFS-LTD and 90% ± 12%; p < 0.05 compared to control for LFS-LTD; Figures 4C and 4D). Thus, like D2 receptors, A2A receptors appear to be acting at or upstream of G_q to modulate both forms of eCB-LTD in indirect-pathway MSNs. We confirmed these results in two different BAC transgenic mouse strains (Drd2-EGFP, target EGFP-positive MSNs; Drd1a-Tmt, target Tmt-negative MSNs), indicating that D2/A2A regulation is robust across multiple mouse lines (Figure S2C).

Dopamine D2 and Adenosine A2A Receptors Modulate eCB-LTD through cAMP/PKA Signaling

We next considered how D2 and A2A receptors modulate eCB mobilization and LTD. Because regulation of eCB biosynthetic pathways by cAMP/PKA signaling is not well established, we first tested whether D2 receptors act to promote eCB-LTD through a reduction in cAMP levels or PKA activation. In this and subsequent experiments, we utilized HFS-LTD to examine the mechanisms regulating eCB-LTD, because this form of LTD remains a standard in the field. To examine whether inhibition
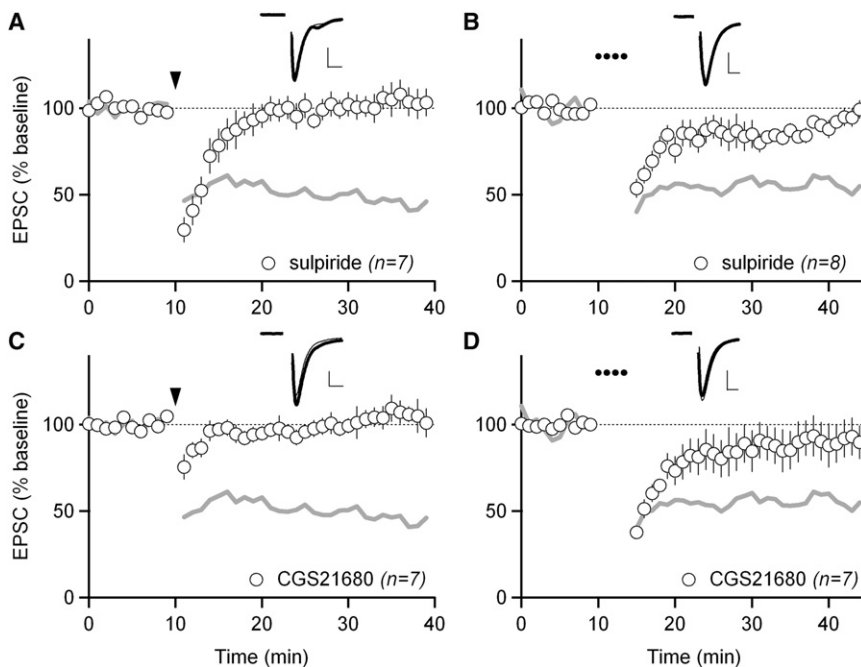
Figure 4. Dopamine D2 and Adenosine A2A Receptors Modulate Both LFS- and HFS-LTD

(A) HFS-LTD in 1 μM of the dopamine D2 receptor antagonist sulpiride. Gray traces in (A) and (C) show control HFS-LTD from Figure 1B for reference. In all panels, scale bars are 100 pA × 5 ms and error bars are SEM.

(B) LFS-LTD in 1 μM sulpiride. Gray traces in (B) and (D) show control LFS-LTD from Figure 1E for reference.

(C) HFS-LTD in 1 μM of the adenosine A2A receptor agonist CGS21680.

(D) LFS-LTD in 1 μM CGS21680.

activating either adenylyl cyclase or PKA would block HFS-LTD when there were no drugs present in the external saline solution. To activate adenylyl cyclase we used the water-soluble (membrane-impermeable) forskolin analog NKH477. To activate PKA we used a membrane-impermeable PKA activator, Sp-8-OH-cAMPS. When either NKH477 or Sp-8-OH-cAMPS were included in our intracellular recording solution, LTD was inhibited (78% ± 5% with NKH477; 89% ± 9% with Sp-8-OH-cAMPS; both $p < 0.05$ compared to control LTD; Figures 5C and 5D). From these experiments, we concluded that increased cAMP/PKA activity inhibits LTD.

D2 and A2A Receptors Regulate Striatal LTD via Regulator of G Protein Signaling 4

How does cAMP/PKA activity block LTD? Because D2 and A2A receptor drugs act on both LFS- and HFS-LTD, they likely act on a common target in both pathways: group I mGluRs or G_q. A particularly attractive candidate for such modulation is regulator of G protein signaling 4 (RGS4). RGS4 is a GTPase-activating protein expressed strongly in MSNs in the dorsolateral striatum, where it is associated with mGluR5 and PLCβ (Gold et al., 1997; Schwendt and McGinty, 2007), its activity is increased by PKA phosphorylation (Huang et al., 2007), and it strongly inhibits signaling through G_q (Saugstad et al., 1998).

To test whether RGS4 is involved in the regulation of LTD by D2 and A2A receptors, we obtained RGS4$^{-/-}$ mice, crossed those mice into our D2-EGFP BAC transgenic line so that we could identify indirect-pathway MSNs, and applied the HFS-LTD induction protocol to indirect-pathway MSNs. In RGS4$^{-/-}$ mice, we observed significant HFS-LTD (66% ± 5%; Figure 6A). If RGS4 is responsible for the connection between D2 and A2A receptor signaling and G_q signaling, then LTD in RGS4$^{-/-}$ mice should occur even in the presence of the D2 antagonist sulpiride or the A2A agonist CGS21680. Indeed, LTD was readily observed in the presence of either drug in RGS4$^{-/-}$ mice (80% ± 6% in sulpiride; 64% ± 7% in CGS21680; Figure 6B).

While genetic knockouts offer complete elimination of the gene product, they also may yield developmental and/or

of cAMP production alone is sufficient to enable eCB-LTD induction, even in the presence of a D2 receptor antagonist, we used a membrane-impermeable adenylyl cyclase inhibitor, ddATP, and a membrane-impermeable inhibitor of PKA, PKI, which were added to our intracellular recording solution. The membrane-impermeability of these drugs limited their effects to the recorded postsynaptic MSN, which allowed us to rule out effects on cAMP/PKA-dependent processes in the presynaptic terminal or in neighboring MSNs or interneurons. With either ddATP or PKI in our intracellular recording solution, we were able to elicit LTD in the presence of sulpiride (69% ± 9% with sulpiride and ddATP; 71% ± 10% with sulpiride and PKI; both $p < 0.05$ compared to LTD in sulpiride alone; Figure 5A).

In contrast to the action of D2 receptors, A2A receptors are G_s-coupled receptors, and we therefore hypothesized that activation of A2A receptors blocks LTD by increasing cAMP/PKA signaling. In support of this hypothesis, we found that reducing cAMP/PKA activity by including either ddATP or PKI in the intracellular recording solution allowed LTD to occur in the presence of A2A agonist CGS21680 (61% ± 4% with CGS21680 and ddATP; 65% ± 7% with CGS21680 and PKI; both $p < 0.05$ compared to LTD in CGS21680 alone; Figure 5B). To verify that the LTD that occurs when cAMP/PKA signaling is inhibited is actually eCB-LTD and not another form of synaptic plasticity, we added the CB1 receptor antagonist AM251 to an extracellular recording solution, which already contained CGS21680 and patched cells with PKI included in the intracellular solution. The addition of AM251 to the extracellular solution blocked LTD (119% ± 16%; $p < 0.05$ compared to LTD with CGS21680 and PKI; Figure S2D), demonstrating that cAMP/PKA inhibition is allowing eCB-LTD to occur.

To further test the hypothesis that increases in cAMP/PKA signaling are sufficient to block LTD, we tested whether directly
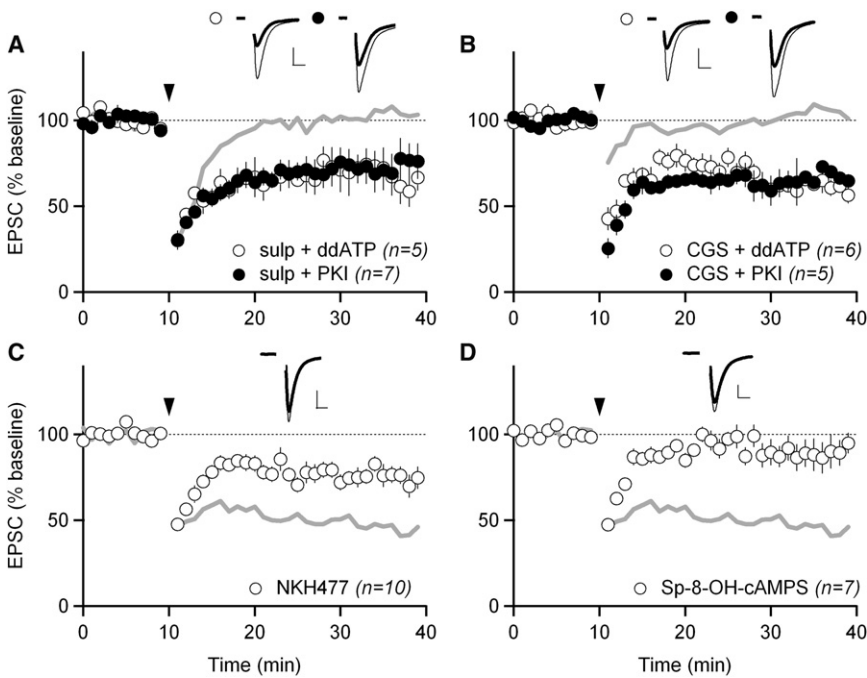
Figure 5. D2 and A2A Receptors Modulate LTD through cAMP/PKA Signaling

(A) HFS-LTD in 1 μM of the D2 receptor antagonist sulpiride and with either 500 nM of the adenylyl cyclase inhibitor ddATP (white circles) or 100 μM of the PKA inhibitor PKI (black circles) in the intracellular solution. Gray trace shows HFS-LTD in sulpiride with no drug in the intracellular solution from Figure 4A for reference. In all panels, scale bars are 100 pA × 5 ms and error bars are SEM.

(B) HFS-LTD in 1 μM of the A2A receptor agonist CGS21680 and with either 500 nM ddATP (white circles) or 100 μM PKI (black circles) in the intracellular solution. Gray trace shows HFS-LTD in CGS21680 with no drug in the intracellular solution from Figure 4C for reference.

(C) HFS-LTD with 10 μM of the adenylyl cyclase activator NKH477 in the intracellular recording solution. Gray traces in C and D show control HFS-LTD from Figure 1B.

(D) HFS-LTD with 0.5–1 mM of the PKA activator Sp-8-OH-cAMPS in the intracellular recording solution.

homeostatic changes. Therefore, we used a recently identified small-molecule inhibitor of RGS4, CCG-63802 (Blazer et al., 2010), to test whether acute inhibition of RGS4 could uncouple LTD from D2 receptors. CCG-63802 was included in the intracellular recording solution to restrict the drug to the postsynaptic neuron, which also allowed us to ask whether RGS4 was acting cell autonomously. With CCG-63802 in the pipette, the magnitude of LTD in control solution and in the presence of sulpiride was indistinguishable (76% ± 10% with CCG-63802; 70% ± 12% with CCG-63802 in sulpiride; Figure 6C). Thus, we conclude that RGS4 is acting acutely in the postsynaptic neuron to modulate LTD.

We also tested whether replacing RGS4 protein in indirect-pathway MSNs from RGS4$^{-/-}$ mice could rescue the modulation of LTD by D2 and A2A receptors. We loaded different concentrations of recombinant RGS4 protein into the pipette and obtained whole-cell recordings from indirect-pathway MSNs in RGS4$^{-/-}$ mice. We found that the effects of loading recombinant RGS4 into the MSN were highly dose-dependent (Figure S4). A low concentration (10 pM) of RGS4 allowed LTD to occur but did not restore the modulation of LTD by D2 and A2A receptors seen in wild-type mice. A higher concentration (50 pM) of RGS4, completely blocked LTD, presumably because G_q signaling was constitutively inhibited by an excess of RGS4. However, an intermediate concentration (25 pM) of RGS4 did not block LTD on its own but enabled LTD to be blocked by either sulpiride or CGS21680 (66% ± 6% with 25 pM RGS4; 84% ± 2% with 25 pM RGS4 in sulpiride; 96% ± 5% with 25 pM RGS4 in CGS21680; LTD with 25 pM RGS4 was significantly different from LTD with 25 pM RGS4 in either sulpiride or CGS21680, p < 0.05; Figure 6D). This result demonstrates that there is a concentration of RGS4 protein that allows for fast, dynamic regulation of its activity,

likely via PKA phosphorylation (Huang et al., 2007). The fact that replacement of RGS4 protein only in the postsynaptic MSN was able to rescue D2 and A2A receptor modulation of LTD in RGS4$^{-/-}$ mice argues against developmental defects contributing to the changes in LTD in the knockout mice, and provides further support for a cell-autonomous action of RGS4.

Indirect-Pathway LTD in RGS4$^{-/-}$ Mice Are Resistant to Dopamine Depletion

The striatum receives dense dopaminergic innervation from the substantia nigra pars compacta, and dopamine is required for proper striatal function. When dopaminergic innervation of the striatum is lost, as occurs in humans with Parkinson's disease, motor function is severely impaired. Similarly, when striatal dopamine is depleted in mice by injecting the toxin 6-OHDA into the medial forebrain bundle (where dopaminergic axons exit the substantia nigra pars compacta), parkinsonian motor behaviors, such as increased immobility and decreased ambulation are observed. At least part of the inhibition of motor function following dopamine depletion may be due to the loss of LTD in indirect-pathway MSNs, which normally requires dopamine D2 receptor activation (Kreitzer and Malenka, 2007). Therefore, we next tested whether LTD could be elicited in indirect-pathway MSNs from dopamine-depleted RGS4$^{-/-}$ mice, where activation of the dopamine D2 receptor is not required for LTD (Figure 6B). We observed normal indirect-pathway HFS-LTD after dopamine depletion with 6-OHDA in RGS4$^{-/-}$ mice (57% ± 10%), whereas in wild-type mice HFS-LTD was absent (97% ± 11%; p < 0.05 compared to RGS4$^{-/-}$; Figure 6E). This finding also held true for LFS-LTD (70% ± 10% for RGS4$^{-/-}$ mice versus 90% ± 5% for wild-type mice; p < 0.05; Figure S1B).
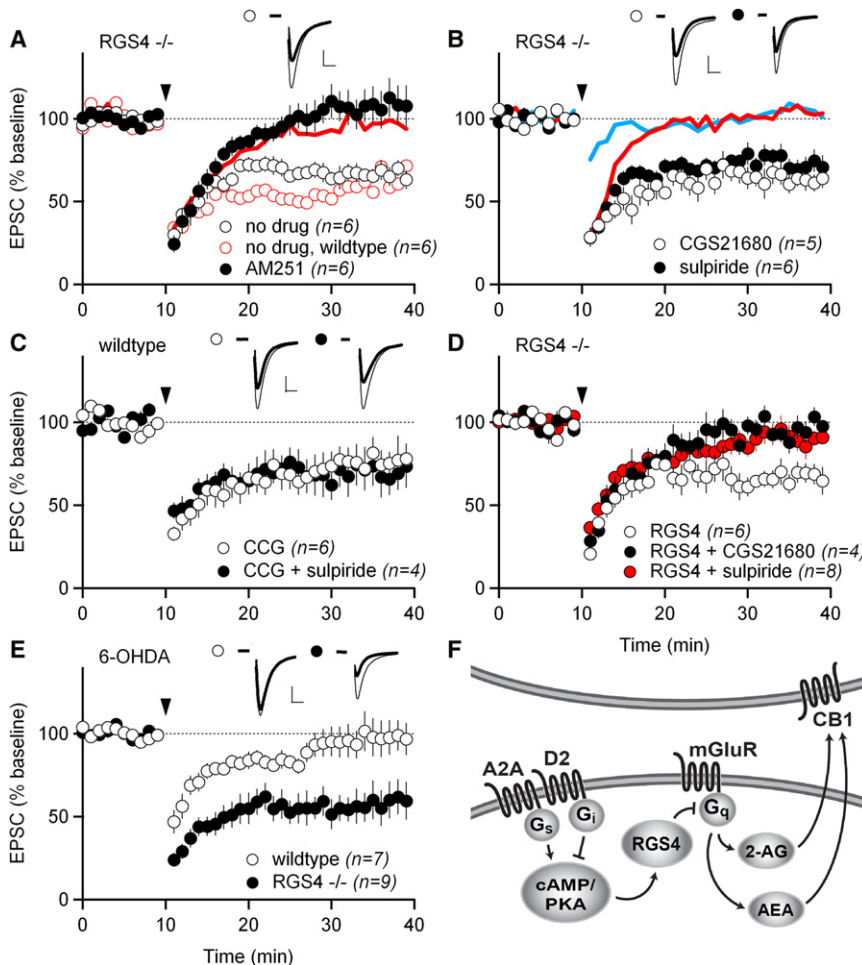
Figure 6. D2 and A2A Receptors Regulate Striatal LTD via Regulator of G Protein Signaling 4

(A) HFS-LTD in RGS4$^{-/-}$ mice in control (no drug) solution (white circles) and in 1 μM of the CB1R antagonist AM251 (black circles). Interleaved HFS-LTD experiments in wild-type mice in control solution are shown as open red circles. The blue trace shows the data from HFS-LTD experiments in wild-type mice in 1 μM AM251 from Figure 1B for reference.

(B) HFS-LTD in RGS4$^{-/-}$ mice in 1 μM of the A2A receptor agonist CGS21680 (white circles) and in 1 μM of the D2 receptor antagonist sulpiride (black circles). The solid lines show HFS-LTD in wild-type mice in 1 μM CGS21680 (blue trace) and in 1 μM sulpiride (red trace) from Figures 4A and 4C.

(C) HFS-LTD with 100 μM of the RGS4 inhibitor CCG-63802 included in the intracellular solution, in combination with either no drug (white circles) or with 1 μM sulpiride (black circles) in the bath.

(D) HFS-LTD in RGS4$^{-/-}$ mice with 25 pM recombinant RGS4 protein included in the intracellular solution and with either no drug (white circles) or with 1 μM CGS21680 (black circles) or with 1 μM sulpiride (red circles) in the bath.

(E) HFS-LTD in dopamine-depleted slices. Slices are from the treated hemisphere of mice injected unilaterally with 6-OHDA in the medial forebrain bundle. Results are shown for wild-type (white circles) and RGS4$^{-/-}$ mice (black circles).

(F) Schematic showing the proposed signaling pathway by which D2 and A2A receptors modulate eCB-LTD. In this model, D2 and A2A receptors oppositely modulate cAMP/PKA. High PKA activity inhibits mGluR-G$_q$ signaling via RGS4. Inhibition of mGluR-G$_q$ signaling prevents the mobilization of both 2-AG and AEA.

RGS4$^{-/-}$ Mice Exhibit Fewer Behavioral Deficits in a Mouse Model of Parkinson's Disease

Loss of indirect-pathway LTD may be a key factor in the overactivity of the indirect pathway—and the concomitant reduction in motor activity—observed after loss of striatal dopamine innervation (DeLong and Wichmann, 2007; Filion and Tremblay, 1991; Obeso et al., 2000). Because RGS4$^{-/-}$ indirect-pathway MSNs, unlike wild-type indirect-pathway MSNs, retain the ability to undergo LTD in dopamine-depleted conditions, we reasoned that RGS4$^{-/-}$ mice might have fewer behavioral deficits following dopamine depletion. To test this hypothesis, we unilaterally injected 6-OHDA into the medial forebrain bundle of RGS4$^{-/-}$ and wild-type mice (Figure 7A). A subset of mice (of each genotype) was injected with an equivalent volume of saline as a control. One week after the injections, each mouse was placed in an open field chamber for 10 min, and its movement was monitored using video tracking software. Wild-type mice injected with 6-OHDA had clear movement deficits when compared to their saline-injected counterparts (Figures 7B–7F). Overall, they moved less distance during the 10 min test period (2,015 ± 178 cm for saline-injected wild-type mice versus 981 ± 178 cm for 6-OHDA-injected wild-type mice; p < 0.05).

In contrast, RGS4$^{-/-}$ mice treated with 6-OHDA, traveled the same distance as their saline-injected counterparts (2,075 ± 85 cm for saline-injected RGS4$^{-/-}$ mice versus 1,618 ± 293 cm for 6-OHDA-injected RGS4$^{-/-}$ mice). RGS4$^{-/-}$ mice treated with 6-OHDA also traveled significantly more distance than wild-type mice treated with 6-OHDA (Figure 7C).

To further dissect the changes in movement that occurred following 6-OHDA injection, we analyzed the percentage of time each mouse spent motionless, ambulating, or making fine movements such as grooming. Wild-type mice that were injected with 6-OHDA spent less time ambulating and more time motionless (freezing) than wild-type mice injected with saline. In contrast, RGS4$^{-/-}$ mice were resistant to the motor deficits displayed by wild-type mice (34% ± 3% of time spent making fine movements, 56% ± 1% ambulating, 10% ± 2% freezing for saline-injected wild-type mice; 22% ± 4% of time spent making fine movements, 27% ± 7% ambulating, 51% ± 11% freezing for 6-OHDA-injected wild-type mice; 25% ± 0.4% of time spent making fine movements, 57% ± 1% ambulating, 18% ± 1% freezing for saline-injected RGS4$^{-/-}$ mice; 23% ± 1% of time spent making fine movements, 50% ± 7% ambulating, 27% ± 7% freezing for 6-OHDA-injected RGS4$^{-/-}$ mice;
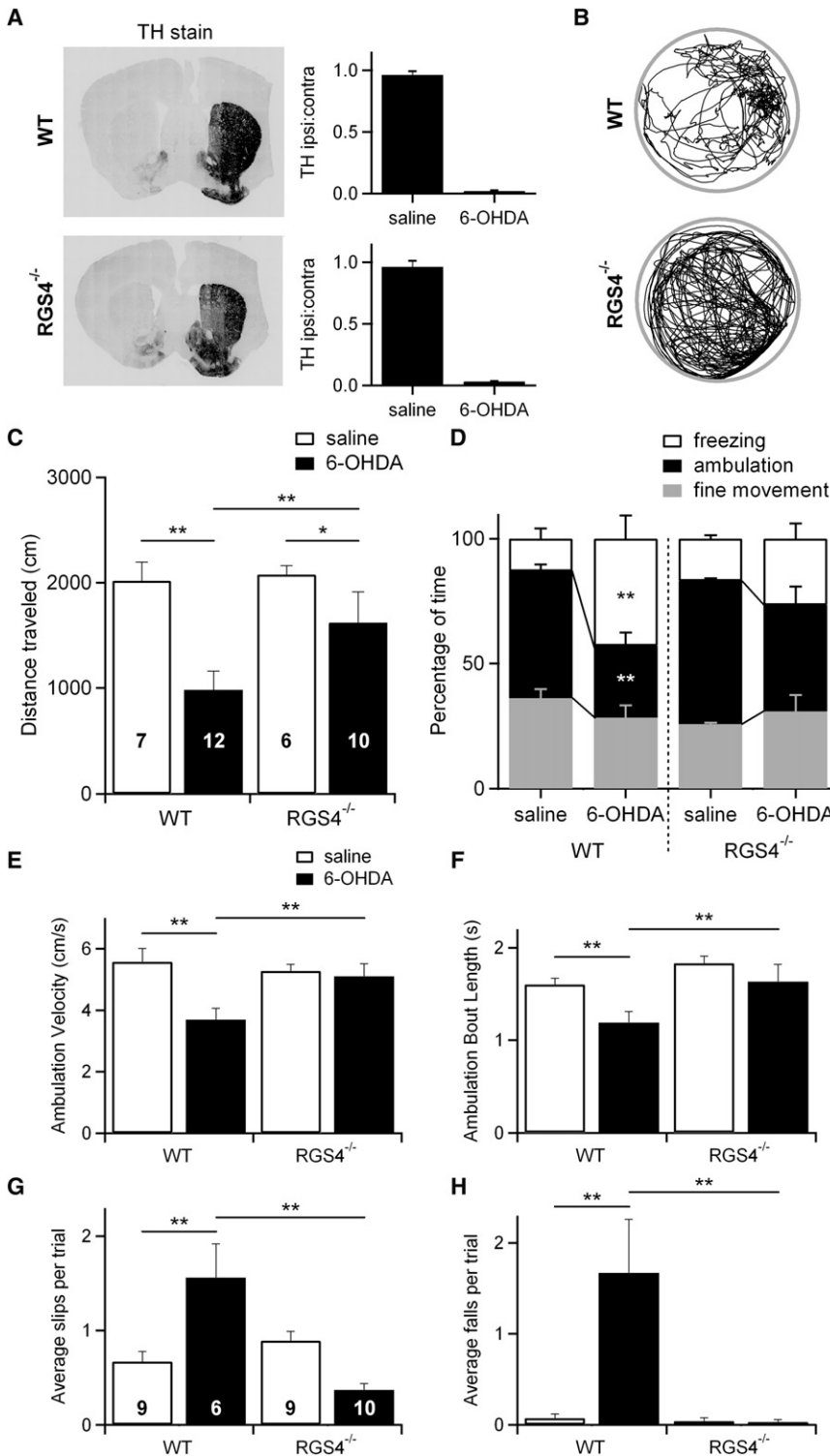
Figure 7. RGS4$^{-/-}$ Mice Have Fewer Behavioral Deficits in a Mouse Model of Parkinson's Disease

(A) Left, example images of coronal brain slices from wild-type (WT) and RGS4$^{-/-}$ mice stained for tyrosine hydroxylase (TH) to verify dopamine depletion following unilateral 6-OHDA injections. Right, quantification of dopamine depletion in all WT and RGS4$^{-/-}$ mice used for behavioral analysis. The intensity of fluorescence on the ipsilateral side was compared to that on the contralateral side for each mouse to yield the TH ipsi:contra ratio.

(B) Examples of the paths taken by dopamine-depleted WT and RGS4$^{-/-}$ mice during the 10 min test period. The example paths shown are from the same mice whose TH staining is shown in (A).

(C) The distances traveled during the test period are shown for saline-injected WT mice (n = 7), 6-OHDA-injected WT mice (n = 12), saline-injected RGS4$^{-/-}$ mice (n = 6), and 6-OHDA-injected RGS4$^{-/-}$ mice (n = 10). Data from the same group of mice is also shown in (D), (E), and (F).

(D) The percentage of time spent freezing, ambulating, or making fine movements is shown for saline-injected WT mice (n = 7), 6-OHDA-injected WT mice (n = 12), saline-injected RGS4$^{-/-}$ mice (n = 6), and 6-OHDA-injected RGS4$^{-/-}$ mice (n = 10).

(E) Average velocity during periods of ambulation is shown for saline-injected WT mice (n = 7), 6-OHDA-injected WT mice (n = 12), saline-injected RGS4$^{-/-}$ mice (n = 6), and 6-OHDA-injected RGS4$^{-/-}$ mice (n = 10).

(F) Average length of an ambulation bout (time spent continuously ambulating before stopping) is shown for saline-injected WT mice (n = 7), 6-OHDA-injected WT mice (n = 12), saline-injected RGS4$^{-/-}$ mice (n = 6), and 6-OHDA-injected RGS4$^{-/-}$ mice (n = 10).

(G) The average number of foot slips per trial on the balance beam is shown for saline-injected WT mice (n = 9), 6-OHDA-injected WT mice (n = 6), saline-injected RGS4$^{-/-}$ mice (n = 9), and 6-OHDA-injected RGS4$^{-/-}$ mice (n = 10). Data from the same group of mice is also shown H. Three additional 6-OHDA-injected WT mice were tested on the balance beam, but failed to perform the task.

(H) The average number of falls per trial on the balance beam is shown for saline-injected WT mice (n = 9), 6-OHDA-injected WT mice (n = 6), saline-injected RGS4$^{-/-}$ mice (n = 9), and 6-OHDA-injected RGS4$^{-/-}$ mice (n = 10).

$*p < 0.05$; $**p < 0.01$.

saline-injected RGS4$^{-/-}$ mice; 5.10 ± 0.41 cm/s for 6-OHDA-injected RGS4$^{-/-}$ mice; Figure 7E) and ambulation bout length (1.60 ± 0.07 s for saline-injected

Figure 7D). RGS4$^{-/-}$ mice were also resistant to deficits observed in wild-type mice in ambulation velocity (5.57 ± 0.44 cm/s for saline-injected wild-type mice; 3.69 ± 0.37 cm/s for 6-OHDA-injected wild-type mice; 5.27 ± 0.22 cm/s for saline-injected wild-type mice; 1.19 ± 0.12 s for 6-OHDA-injected wild-type mice; 1.83 ± 0.08 s for saline-injected RGS4$^{-/-}$ mice; 1.63 ± 0.19 s for 6-OHDA-injected RGS4$^{-/-}$ mice; Figure 7F). Despite improved overall movement, unilaterally 6-OHDA-injected

RGS4$^{-/-}$ and wild-type mice had similar ipsilateral rotational biases (Figure S5), perhaps due to remaining dopamine-dependent imbalances in the function of the contralateral and ipsilateral striatum. Bilateral injection of 6-OHDA caused more severe behavioral deficits than unilateral injection, but the differences between wild-type and RGS4$^{-/-}$ mice were quite similar to those observed in unilaterally injected mice (Figure S6).

Although the open field results were striking, distance traveled is not a stringent test of motor coordination. To test for motor coordination, we used a balance beam task in which mice must traverse a narrow, elevated beam to reach a dark, enclosed box (Carter et al., 1999; Fleming et al., 2004). Each mouse was tested on three trials and foot slips on the beam as well as falls off the beam were counted for each trial. Saline-injected wild-type and RGS4$^{-/-}$ mice both appeared similarly coordinated on this task; they made very few foot slips and almost never fell off the beam (0.67 ± 0.11 slips and 0.07 ± 0.05 falls per trial for wild-type mice, 0.89 ± 0.09 slips and 0.03 ± 0.04 falls per trial for RGS4$^{-/-}$ mice; Figures 7G and 7H). 6-OHDA-injected wild-type mice, however, were impaired. Of nine mice tested, three could not perform the task at all. The six mice that did traverse the beam had more foot slips and also fell off the beam significantly more than their saline-injected counterparts (1.59 ± 0.36 slips and 1.67 ± 0.59 falls per trial; Figure 7H). They usually fell at least once and often more than once per trial, meaning they could not have completed the task without being placed back onto the beam by the experimenter. In contrast, 6-OHDA-injected RGS4$^{-/-}$ mice almost never slipped or fell on the balance beam (0.33 ± 0.08 slips and 0.09 ± 0.06 falls per trial; Figure 7H). There were no significant differences in slipping or falling between 6-OHDA-injected RGS4$^{-/-}$ mice and their saline-injected counterparts and indeed, 6-OHDA-injected RGS4$^{-/-}$ mice performed significantly better than 6-OHDA-injected wild-type mice. These data indicate that RGS4$^{-/-}$ mice are significantly more coordinated following dopamine depletion than wild-type mice. Furthermore, our open field and balance beam data all support the conclusion that RGS4 is a critical link between loss of dopamine, dysregulation of striatal eCB-LTD, and motor impairments.

DISCUSSION

In this study, we characterized a novel mechanism linking dopamine D2 and adenosine A2A receptor signaling to mobilization of eCBs through the GTPase-accelerating protein RGS4. We found that eCB-LTD can be induced by engaging either of two distinct biosynthetic pathways, both of which require D2 receptor activation and are inhibited by A2A receptor activation. This modulation of eCB-LTD by D2 and A2A receptors requires RGS4, which is phosphorylated by PKA (Huang et al., 2007) and inhibits mGluR-G$_q$ signaling (Saugstad et al., 1998). RGS4 is therefore a key link between dopamine signaling, synaptic plasticity, and motor behavior, and may be a promising non-dopaminergic target for modulating basal ganglia circuitry.

Two Distinct Forms of Indirect-Pathway eCB-LTD
Our finding of two distinct forms of eCB-LTD (HFS-LTD and LFS-LTD) in the same cell type both clarifies previous findings and raises new questions. Our data agree with previous studies indicating that AEA is the eCB mediating HFS-LTD while highlighting the importance of PLD for its production (Ade and Lovinger, 2007; Kreitzer and Malenka, 2007). However, other studies of striatal eCB-LTD have indicated that 2-AG is the eCB that mediates striatal eCB-LTD (Fino et al., 2010; Lerner et al., 2010). Indeed, we confirm that 2-AG can also mediate eCB-LTD, given the right stimulation frequency and duration, thus helping to resolve some of the apparent conflicts in the literature. Additionally, our LFS-LTD data fit well with a previous study of striatal LTD using low-frequency stimulation (Ronesi and Lovinger, 2005), which until now was difficult to reconcile with studies of HFS-LTD. Like this LTD, which was induced by 5 min of continuous 10 Hz stimulation, our LFS-LTD is prevented by blockers of CB1 receptors and D2 receptors, but not by L-VGCC blockers or by calcium chelation with BAPTA. Together with our data, these findings demonstrate that eCB-LTD can be calcium-independent, most likely because PLCβ can be sufficiently activated by prolonged group I mGluR activation alone.

Dopamine D2 and Adenosine A2A Receptors in Indirect-Pathway MSNs Modulate LTD Induction
Both HFS-LTD and LFS-LTD are modulated by dopamine D2 receptors and adenosine A2A receptors and this modulation of LTD appears to be important for regulating motor function (Kreitzer and Malenka, 2007; Lerner et al., 2010). Here we provide the first evidence of a specific mechanism by which D2 and A2A receptor modulation of LTD occurs, via cAMP/PKA mediated regulation of RGS4 activity. While our experiments argue that D2 and A2A receptors regulate LTD induction mainly via their downstream signaling pathways, we cannot rule out a role for physical interactions of D2 and A2A receptors in the membrane, which have been reported (for review see Fuxe et al., 2005, 2007), though not studied in the context of LTD. D2 and A2A receptors appear to regulate cAMP accumulation in MSNs primarily by acting on adenylyl cyclase 5 (AC5), a striatal-enriched form of adenylyl cyclase, since mice lacking AC5 have impaired striatal synaptic plasticity. Specifically, although excitatory synapses onto MSNs from AC5$^{-/-}$ mice respond normally to the group I mGluR agonist DHPG, this response cannot be enhanced by D2 receptor activation as it can in wild-type mice (Kheirbek et al., 2009).

Some controversy exists in the literature regarding the site of the D2 and A2A receptors that control eCB release and LTD, with some groups arguing that D2/A2A expression in cholinergic interneurons is critical for regulating LTD (Tozzi et al., 2011; Wang et al., 2006). Importantly, our experiments demonstrate that D2 and A2A receptors exert their action in the postsynaptic MSN and not in other cell types such as cholinergic interneurons. All of the drugs we used to manipulate cAMP/PKA activity are membrane-impermeable and were delivered only to the postsynaptic MSN via the recording pipette. We also delivered both CCG-63802 (the RGS4 inhibitor) and recombinant RGS4 protein only to MSNs, via the recording pipette. Thus, we conclude that RGS4 acts cell autonomously in the MSNs and not through actions in interneurons, neighboring MSNs, or presynaptic axons.

RGS4 and Neurological Disease

Regulators of G protein signaling (RGSs) are GTPase-activating proteins, which negatively regulate G proteins by accelerating their inactivation. RGS4 is an RGS that is highly expressed in striatum (Gold et al., 1997) and there is evidence linking changes in RGS4 function with a variety of neurological diseases involving the striatum, including Parkinson's disease, Huntington's disease, and addiction (Ding et al., 2006; Geurts et al., 2003; Kuhn et al., 2007; Schwendt et al., 2007; Schwendt and McGinty, 2007; Zhang et al., 2005). Here, we find that RGS4$^{-/-}$ mice have dopamine-independent indirect-pathway eCB-LTD and show fewer behavioral deficits following dopamine depletion with 6-OHDA, a mouse model of Parkinson's disease. However, our behavioral experiments provide only a glimpse into the motor function of dopamine-depleted RGS4$^{-/-}$ mice. A more comprehensive evaluation of parkinsonism in RGS4$^{-/-}$ mice will be required to illuminate which particular aspects of movement are critically regulated by eCB-LTD.

Loss of RGS4 in direct-pathway MSNs and cholinergic interneurons (Ding et al., 2006) may also be contributing to the improved phenotype of RGS4$^{-/-}$ mice following dopamine depletion since RGS4 is expressed in all of these cell types (Taymans et al., 2004). Although we focused on dissecting the mechanisms underlying indirect-pathway LTD in this paper, Parkinson's disease pathophysiology is complex and the effects of RGS4 loss on other cell types will be an important topic for future study. Future experiments examining the effects of knocking out RGS4 selectively in different cell types will be useful in clarifying the roles that RGS4 plays in these different contexts.

The reduced behavioral deficits following dopamine depletion in RGS4$^{-/-}$ mice indicate that RGS4 inhibition may be an effective nondopaminergic strategy for treating Parkinson's disease. Although downregulation of RGS4 may be an adaptive change that already takes place in response to dopamine depletion (Geurts et al., 2003; Zhang et al., 2005), our findings indicate that further downregulation is beneficial. In this study, we were able to use an existing compound, CCG-63802, at a relatively high concentration (100 μM) delivered directly to single neurons via the intracellular recording solution to inhibit RGS4 activity. Although helpful for our study, administration of CCG-63802 or related analogs in vivo is not likely to be an effective strategy, due to the sensitivity of these compounds to reducing conditions (Blazer et al., 2011). Hopefully, RGS4 inhibitors with suitable characteristics for clinical use are on the horizon and can be tested as Parkinson's disease therapeutics or for other conditions in which RGS4 is involved.

EXPERIMENTAL PROCEDURES

All procedures involving animals were approved by the UCSF Institutional Animal Care and Use Committee (IACUC). See Supplemental Experimental Procedures for detailed methods.

Electrophysiology

Coronal brain slices (300 μm) were prepared from Drd2-GFP$^{+/-}$ (or Drd1-tmt$^{+/-}$ in Figure S2C) BAC transgenic mice (P21–35). Where stated mice were also RGS4$^{-/-}$. Whole-cell voltage-clamp recordings from indirect-pathway MSNs were obtained from visually identified GFP-positive or tmt-negative MSNs in dorsolateral striatum at a temperature of 30°C–32°C,

with picrotoxin (50 μM) present to suppress GABA$_A$-mediated currents. MSNs were held at −70mV, and excitatory postsynaptic currents (EPSCs) were evoked by intrastriatal microstimulation with a saline-filled glass pipette placed 50–100 μm dorsolateral of the recorded neuron. Test pulses were given every 20 s. To evoke LTD, MSNs were stimulated at 20 or 100 Hz for 1 s, paired with postsynaptic depolarization to −10mV, at 10 s intervals. For HFS-LTD, 100 Hz stimulation was repeated four times. For LFS-LTD, 20 Hz stimulation was repeated 30 times. The magnitude of LTD was calculated as the average EPSC amplitude at 30–40 min as a percentage of the average baseline (0–10 min) EPSC amplitude and reported in the text as the percentage of baseline ± SEM. Statistical significance was evaluated using two-tailed unpaired t tests.

6-OHDA Injections

Mice were injected with 6-OHDA into the medial forebrain bundle at 3 weeks of age (for electrophysiology) or 7 weeks of age (for behavior). Electrophysiology was performed 4–6 days following injection. Behavior was performed 6–7 days following unilateral injection or 4 days following bilateral injection.

Open Field Behavior

Activity in an open field was tracked using ETHOVISION 7 software (Noldus, Leesburg, VA, USA). Ambulation was defined as movement of the center of mass greater than 2 cm/s. Fine Movement was defined as movement of the center of mass less than 1.75 cm/s with greater than 2% of pixels in the image changing. Freezing was defined as movement of the center of mass of less than 1.75 cm/s with less than 2% of pixels in the image changing. Statistical significance was evaluated using a two-way ANOVA with Tukey's HSD.

Balance Beam Behavior

Mice were trained to walk across a rectangular 0.5 cm thick beam. Slips on and falls off the balance beam were recorded for later analysis. Statistical significance was evaluated using a two-way ANOVA with Tukey's HSD.

Tyrosine Hydroxylase Staining

Tissue was fixed overnight in 4% PFA and cut into 30 μm sections on a SM2010R freezing microtome (Leica, Wetzlar, Germany). Tissue was blocked with 10% normal donkey serum and permeabilized with 0.1% Triton X-100. Primary antibody incubation was performed at 4°C for 24 hr, using rabbit anti-TH (1:200; Pel-Freeze, Rogers, AR, USA). Secondary antibody, goat anti-rabbit (1:500, Vector Labs, Burlingame, CA, USA) was incubated for 1 hr at room temperature. Images were taken on a 6D epifluorescent microscope (Nikon, Shinjuku, Tokyo, Japan) and quantified using ImageJ software.

SUPPLEMENTAL INFORMATION

Supplemental Information includes six figures and Supplemental Experimental Procedures and can be found with this article online at doi:10.1016/j.neuron.2011.11.015.

REFERENCES

Ade, K.K., and Lovinger, D.M. (2007). Anandamide regulates postnatal development of long-term synaptic plasticity in the rat dorsolateral striatum. J. Neurosci. 27, 2403–2409.

Adermark, L., and Lovinger, D.M. (2007). Combined activation of L-type Ca2+ channels and synaptic transmission is sufficient to induce striatal long-term depression. J. Neurosci. 27, 6781–6787.

Ahn, K., McKinney, M.K., and Cravatt, B.F. (2008). Enzymatic pathways that regulate endocannabinoid signaling in the nervous system. Chem. Rev. 108, 1687–1707.

Bence-Hanulec, K.K., Marshall, J., and Blair, L.A. (2000). Potentiation of neuronal L calcium channels by IGF-1 requires phosphorylation of the alpha1 subunit on a specific tyrosine residue. Neuron 27, 121–131.

Bence, K., Ma, W., Kozasa, T., and Huang, X.Y. (1997). Direct stimulation of Bruton's tyrosine kinase by G(q)-protein alpha-subunit. Nature 389, 296–299.

Blazer, L.L., Roman, D.L., Chung, A., Larsen, M.J., Greedy, B.M., Husbands, S.M., and Neubig, R.R. (2010). Reversible, allosteric small-molecule inhibitors of regulator of G protein signaling proteins. Mol. Pharmacol. 78, 524–533.

Blazer, L.L., Zhang, H., Casey, E.M., Husbands, S.M., and Neubig, R.R. (2011). A nanomolar-potency small molecule inhibitor of regulator of G-protein signaling proteins. Biochemistry 50, 3181–3192.

Bolam, J.P., Hanley, J.J., Booth, P.A., and Bevan, M.D. (2000). Synaptic organisation of the basal ganglia. J. Anat. 196, 527–542.

Calabresi, P., Pisani, A., Mercuri, N.B., and Bernardi, G. (1994). Post-receptor mechanisms underlying striatal long-term depression. J. Neurosci. 14, 4871–4881.

Calabresi, P., Saiardi, A., Pisani, A., Baik, J.H., Centonze, D., Mercuri, N.B., Bernardi, G., and Borrelli, E. (1997). Abnormal synaptic plasticity in the striatum of mice lacking dopamine D2 receptors. J. Neurosci. 17, 4536–4544.

Carter, R.J., Lione, L.A., Humby, T., Mangiarini, L., Mahal, A., Bates, G.P., Dunnett, S.B., and Morton, A.J. (1999). Characterization of progressive motor deficits in mice transgenic for the human Huntington's disease mutation. J. Neurosci. 19, 3248–3257.

Chavis, P., Fagni, L., Lansman, J.B., and Bockaert, J. (1996). Functional coupling between ryanodine receptors and L-type calcium channels in neurons. Nature 382, 719–722.

Choi, S., and Lovinger, D.M. (1997). Decreased probability of neurotransmitter release underlies striatal long-term depression and postnatal development of corticostriatal synapses. Proc. Natl. Acad. Sci. USA 94, 2665–2670.

DeLong, M.R., and Wichmann, T. (2007). Circuits and circuit disorders of the basal ganglia. Arch. Neurol. 64, 20–24.

Ding, J., Guzman, J.N., Tkatch, T., Chen, S., Goldberg, J.A., Ebert, P.J., Levitt, P., Wilson, C.J., Hamm, H.E., and Surmeier, D.J. (2006). RGS4-dependent attenuation of M4 autoreceptor function in striatal cholinergic interneurons following dopamine depletion. Nat. Neurosci. 9, 832–842.

Filion, M., and Tremblay, L. (1991). Abnormal spontaneous activity of globus pallidus neurons in monkeys with MPTP-induced parkinsonism. Brain Res. 547, 142–151.

Fino, E., Paille, V., Cui, Y., Morera-Herreras, T., Deniau, J.M., and Venance, L. (2010). Distinct coincidence detectors govern the corticostriatal spike timing-dependent plasticity. J. Physiol. 588, 3045–3062.

Fleming, S.M., Salcedo, J., Fernagut, P.O., Rockenstein, E., Masliah, E., Levine, M.S., and Chesselet, M.F. (2004). Early and progressive sensorimotor anomalies in mice overexpressing wild-type human alpha-synuclein. J. Neurosci. 24, 9434–9440.

Fuxe, K., Ferré, S., Canals, M., Torvinen, M., Terasmaa, A., Marcellino, D., Goldberg, S.R., Staines, W., Jacobsen, K.X., Lluis, C., et al. (2005). Adenosine A2A and dopamine D2 heteromeric receptor complexes and their function. J. Mol. Neurosci. 26, 209–220.

Fuxe, K., Marcellino, D., Genedani, S., and Agnati, L. (2007). Adenosine A(2A) receptors, dopamine D(2) receptors and their interactions in Parkinson's disease. Mov. Disord. 22, 1990–2017.

Gao, Y., Vasilyev, D.V., Goncalves, M.B., Howell, F.V., Hobbs, C., Reisenberg, M., Shen, R., Zhang, M.Y., Strassle, B.W., Lu, P., et al. (2010). Loss of retrograde endocannabinoid signaling and reduced adult neurogenesis in diacylglycerol lipase knock-out mice. J. Neurosci. 30, 2017–2024.

Geurts, M., Maloteaux, J.M., and Hermans, E. (2003). Altered expression of regulators of G-protein signaling (RGS) mRNAs in the striatum of rats undergoing dopamine depletion. Biochem. Pharmacol. 66, 1163–1170.

Giuffrida, A., Parsons, L.H., Kerr, T.M., Rodríguez de Fonseca, F., Navarro, M., and Piomelli, D. (1999). Dopamine activation of endogenous cannabinoid signaling in dorsal striatum. Nat. Neurosci. 2, 358–363.

Gold, S.J., Ni, Y.G., Dohlman, H.G., and Nestler, E.J. (1997). Regulators of G-protein signaling (RGS) proteins: region-specific expression of nine subtypes in rat brain. J. Neurosci. 17, 8024–8037.

Graybiel, A.M., Aosaki, T., Flaherty, A.W., and Kimura, M. (1994). The basal ganglia and adaptive motor control. Science 265, 1826–1831.

Hashimotodani, Y., Ohno-Shosaku, T., Tsubokawa, H., Ogata, H., Emoto, K., Maejima, T., Araishi, K., Shin, H.S., and Kano, M. (2005). Phospholipase Cbeta serves as a coincidence detector through its Ca2+ dependency for triggering retrograde endocannabinoid signal. Neuron 45, 257–268.

Henkels, K.M., Peng, H.J., Frondorf, K., and Gomez-Cambronero, J. (2010). A comprehensive model that explains the regulation of phospholipase D2 activity by phosphorylation-dephosphorylation. Mol. Cell. Biol. 30, 2251–2263.

Hikosaka, O., Takikawa, Y., and Kawagoe, R. (2000). Role of the basal ganglia in the control of purposive saccadic eye movements. Physiol. Rev. 80, 953–978.

Huang, J., Zhou, H., Mahavadi, S., Sriwai, W., and Murthy, K.S. (2007). Inhibition of Galphaq-dependent PLC-beta1 activity by PKG and PKA is mediated by phosphorylation of RGS4 and GRK2. Am. J. Physiol. Cell Physiol. 292, C200–C208.

Hubbard, K.B., and Hepler, J.R. (2006). Cell signalling diversity of the Gqalpha family of heterotrimeric G proteins. Cell. Signal. 18, 135–150.

Jung, K.M., Mangieri, R., Stapleton, C., Kim, J., Fegley, D., Wallace, M., Mackie, K., and Piomelli, D. (2005). Stimulation of endocannabinoid formation in brain slice cultures through activation of group I metabotropic glutamate receptors. Mol. Pharmacol. 68, 1196–1202.

Kheirbek, M.A., Britt, J.P., Beeler, J.A., Ishikawa, Y., McGehee, D.S., and Zhuang, X. (2009). Adenylyl cyclase type 5 contributes to corticostriatal plasticity and striatum-dependent learning. J. Neurosci. 29, 12115–12124.

Kitada, T., Pisani, A., Porter, D.R., Yamaguchi, H., Tscherter, A., Martella, G., Bonsi, P., Zhang, C., Pothos, E.N., and Shen, J. (2007). Impaired dopamine release and synaptic plasticity in the striatum of PINK1-deficient mice. Proc. Natl. Acad. Sci. USA 104, 11441–11446.

Kitada, T., Pisani, A., Karouani, M., Haburcak, M., Martella, G., Tscherter, A., Platania, P., Wu, B., Pothos, E.N., and Shen, J. (2009). Impaired dopamine release and synaptic plasticity in the striatum of parkin-/- mice. J. Neurochem. 110, 613–621.

Kreitzer, A.C., and Malenka, R.C. (2005). Dopamine modulation of state-dependent endocannabinoid release and long-term depression in the striatum. J. Neurosci. 25, 10537–10545.

Kreitzer, A.C., and Malenka, R.C. (2007). Endocannabinoid-mediated rescue of striatal LTD and motor deficits in Parkinson's disease models. Nature 445, 643–647.

Kreitzer, A.C., and Malenka, R.C. (2008). Striatal plasticity and basal ganglia circuit function. Neuron 60, 543–554.

Kuhn, A., Goldstein, D.R., Hodges, A., Strand, A.D., Sengstag, T., Kooperberg, C., Becanovic, K., Pouladi, M.A., Sathasivam, K., Cha, J.H., et al. (2007). Mutant huntingtin's effects on striatal gene expression in mice recapitulate changes observed in human Huntington's disease brain and do not differ with mutant huntingtin length or wild-type huntingtin dosage. Hum. Mol. Genet. 16, 1845–1861.

Kurz, A., Double, K.L., Lastres-Becker, I., Tozzi, A., Tantucci, M., Bockhart, V., Bonin, M., García-Arencibia, M., Nuber, S., Schlaudraff, F., et al. (2010).

A53T-alpha-synuclein overexpression impairs dopamine signaling and striatal synaptic plasticity in old mice. PLoS ONE 5, e11464.

Lerner, T.N., Horne, E.A., Stella, N., and Kreitzer, A.C. (2010). Endocannabinoid signaling mediates psychomotor activation by adenosine A2A antagonists. J. Neurosci. 30, 2160–2164.

Lerner, T.N., and Kreitzer, A.C. (2011). Neuromodulatory control of striatal plasticity and behavior. Curr. Opin. Neurobiol. 21, 322–327.

Leung, D., Saghatelian, A., Simon, G.M., and Cravatt, B.F. (2006). Inactivation of N-acyl phosphatidylethanolamine phospholipase D reveals multiple mechanisms for the biosynthesis of endocannabinoids. Biochemistry 45, 4720–4726.

Obeso, J.A., Rodriguez-Oroz, M.C., Rodriguez, M., Macias, R., Alvarez, L., Guridi, J., Vitek, J., and DeLong, M.R. (2000). Pathophysiologic basis of surgery for Parkinson's disease. Neurology 55 (12, Suppl 6), S7–S12.

Packard, M.G., and Knowlton, B.J. (2002). Learning and memory functions of the Basal Ganglia. Annu. Rev. Neurosci. 25, 563–593.

Peterson, D.A., Sejnowski, T.J., and Poizner, H. (2010). Convergent evidence for abnormal striatal synaptic plasticity in dystonia. Neurobiol. Dis. 37, 558–573.

Piomelli, D. (2003). The molecular logic of endocannabinoid signalling. Nat. Rev. Neurosci. 4, 873–884.

Ronesi, J., and Lovinger, D.M. (2005). Induction of striatal long-term synaptic depression by moderate frequency activation of cortical afferents in rat. J. Physiol. 562, 245–256.

Saugstad, J.A., Marino, M.J., Folk, J.A., Hepler, J.R., and Conn, P.J. (1998). RGS4 inhibits signaling by group I metabotropic glutamate receptors. J. Neurosci. 18, 905–913.

Schwendt, M., and McGinty, J.F. (2007). Regulator of G-protein signaling 4 interacts with metabotropic glutamate receptor subtype 5 in rat striatum: relevance to amphetamine behavioral sensitization. J. Pharmacol. Exp. Ther. 323, 650–657.

Schwendt, M., Hearing, M.C., See, R.E., and McGinty, J.F. (2007). Chronic cocaine reduces RGS4 mRNA in rat prefrontal cortex and dorsal striatum. Neuroreport 18, 1261–1265.

Shen, W., Flajolet, M., Greengard, P., and Surmeier, D.J. (2008). Dichotomous dopaminergic control of striatal synaptic plasticity. Science 321, 848–851.

Sung, K.W., Choi, S., and Lovinger, D.M. (2001). Activation of group I mGluRs is necessary for induction of long-term depression at striatal synapses. J. Neurophysiol. 86, 2405–2412.

Surmeier, D.J., Plotkin, J., and Shen, W. (2009). Dopamine and synaptic plasticity in dorsal striatal circuits controlling action selection. Curr. Opin. Neurobiol. 19, 621–628.

Tanimura, A., Yamazaki, M., Hashimotodani, Y., Uchigashima, M., Kawata, S., Abe, M., Kita, Y., Hashimoto, K., Shimizu, T., Watanabe, M., et al. (2010). The endocannabinoid 2-arachidonoylglycerol produced by diacylglycerol lipase alpha mediates retrograde suppression of synaptic transmission. Neuron 65, 320–327.

Taylor, S.J., Chae, H.Z., Rhee, S.G., and Exton, J.H. (1991). Activation of the beta 1 isozyme of phospholipase C by alpha subunits of the Gq class of G proteins. Nature 350, 516–518.

Taymans, J.M., Kia, H.K., Claes, R., Cruz, C., Leysen, J., and Langlois, X. (2004). Dopamine receptor-mediated regulation of RGS2 and RGS4 mRNA differentially depends on ascending dopamine projections and time. Eur. J. Neurosci. 19, 2249–2260.

Tozzi, A., Tscherter, A., Belcastro, V., Tantucci, M., Costa, C., Picconi, B., Centonze, D., Calabresi, P., and Borsini, F. (2007). Interaction of A2A adenosine and D2 dopamine receptors modulates corticostriatal glutamatergic transmission. Neuropharmacology 53, 783–789.

Tozzi, A., de Iure, A., Di Filippo, M., Tantucci, M., Costa, C., Borsini, F., Ghiglieri, V., Giampà, C., Fusco, F.R., Picconi, B., and Calabresi, P. (2011). The distinct role of medium spiny neurons and cholinergic interneurons in the D_2/A_2A receptor interaction in the striatum: implications for Parkinson's disease. J. Neurosci. 31, 1850–1862.

Uchigashima, M., Narushima, M., Fukaya, M., Katona, I., Kano, M., and Watanabe, M. (2007). Subcellular arrangement of molecules for 2-arachidonoyl-glycerol-mediated retrograde signaling and its physiological contribution to synaptic modulation in the striatum. J. Neurosci. 27, 3663–3676.

Wang, Z., Kai, L., Day, M., Ronesi, J., Yin, H.H., Ding, J., Tkatch, T., Lovinger, D.M., and Surmeier, D.J. (2006). Dopaminergic control of corticostriatal long-term synaptic depression in medium spiny neurons is mediated by cholinergic interneurons. Neuron 50, 443–452.

Yin, H.H., and Knowlton, B.J. (2006). The role of the basal ganglia in habit formation. Nat. Rev. Neurosci. 7, 464–476.

Yin, H.H., and Lovinger, D.M. (2006). Frequency-specific and D2 receptor-mediated inhibition of glutamate release by retrograde endocannabinoid signaling. Proc. Natl. Acad. Sci. USA 103, 8251–8256.

Zhang, Y., James, M., Middleton, F.A., and Davis, R.L. (2005). Transcriptional analysis of multiple brain regions in Parkinson's disease supports the involvement of specific protein processing, energy metabolism, and signaling pathways, and suggests novel disease mechanisms. Am. J. Med. Genet. B. Neuropsychiatr. Genet. 137B, 5–16.